Int. J. Therm. Sci. (2000) 39, 30–38

S1290-0729(00)00197-5/FLA

Analysis of the process characteristics of an absorption heat transformer with compact heat exchangers and the mixture TFE–E181

Andreas Genssle [a]*, Karl Stephan [b]*

[a] *Robert Bosch GmbH, Forschung und Vorausentwicklung FV/PLO1, Postfach 30 02 40, 70442 Stuttgart, Germany*

[b] *Institut für Technische Thermodynamik und Thermische Verfahrenstechnik, Universität Stuttgart, Pfaffenwaldring 9, 70550 Stuttgart, Germany*

(Received 15 July 1999, accepted 9 September 1999)

Abstract — In the project described in this paper an experimental rig for a one-stage absorption heat transformer was designed and constructed. One aim of the project was to reduce the investment costs for the apparatus. This incorporates new and less expensive compact brazed plate heat exchangers for generator, evaporator, condenser and solution heat exchanger. The absorber was designed as a helical coil pipe absorber, where the weak solution trickles down as a falling film outside of the coil. The tests of the equipment involved measurements using a mixture of trifluorethanol (TFE) and tetraethyleneglycoldimethylether (E181). The process characteristics were investigated for different temperatures of the rich solution leaving the absorber. Experimental results are presented and compared with the results of a computer simulation model. Additionally the model was used to compare the COP of the heat transformation process with the mixtures lithium bromide–water (LiBr–H_2O) and ammonia–water (NH_3–H_2O). Furthermore, the overall heat and mass transfer coefficients for the plate heat exchangers and the falling film absorber were evaluated and compared with those of shell and tube heat exchangers. © 2000 Éditions scientifiques et médicales Elsevier SAS

absorption heat transformer / plate heat exchanger / trifluoroethanol / E181 / absorber / experiments / simulation / heat and mass transfer / heat transfer coefficient / mass transfer coefficient

Nomenclature

A	area	m^2
a_V	volumetric area	m^{-1}
c_p	specific heat capacity	$J{\cdot}g^{-1}{\cdot}K^{-1}$
D	diffusion coefficient	$m^2{\cdot}s^{-1}$
f	specific solution ratio	
f_{re}	specific reflux ratio	
k	overall heat transfer coefficient	$W{\cdot}m^{-2}{\cdot}K^{-1}$
$\dot{m}$	mass flow	$kg{\cdot}s^{-1}$
p	pressure	Pa
$\dot{Q}$	heat flow	W
Re_F	Reynolds number of the falling film	
T	temperature	K
U	covered tube circumference	m

Greek symbols

β	overall mass transfer coefficient	$kg{\cdot}m^{-2}{\cdot}s^{-1}$
$\Delta\vartheta$	logarithmic mean temperature difference	K
λ	thermal conductivity	$W{\cdot}m^{-1}{\cdot}K^{-1}$
η	dynamic viscosity	$kg{\cdot}m^{-1}{\cdot}s^{-1}$
Θ	temperature difference	K
ρ	density	$kg{\cdot}m^{-3}$
ΔT	temperature lift	K
$\Delta\xi$	mass fraction spread	
$\Delta\Upsilon$	logarithmic mean mass fraction difference	
ψ	heat ratio	
ψ	mass fraction TFE	
ζ	coefficient of performance (COP)	

Subscripts

A	absorber
C	condenser
E	evaporator
F	film
G	generator

* Correspondence and reprints.
Andreas.Genssle@de.bosch.com, stephan@itt.uni-stuttgart.de

i inlet
o outlet
R refrigerant
r rich solution
re reflux
V volumetric
w weak solution

Superscripts

L liquid

1. INTRODUCTION

Heat transformation is a promising method for heat recovery. It enables a fraction of the waste heat to be transformed from a moderate temperature level T_1 to a higher temperature T_2 in the absorber. The heat can be fed back into a process, whilst the excess heat will be released at a lower temperature T_0. In the process trifluorethanol (TFE) served as refrigerant and tetraethyleneglycoldimethylether (E181) as absorbant. This binary mixture has been investigated intensively by Seher and Stephan [1, 2], Hengerer and Stephan [3] and Seher [4]. Coronas et al. [5] investigated also the thermophysical properties of this mixture and proved in a theoretical study TFE–E181 to be useful for absorption heat transformers and absorption heat pumps [6–8]. The most often used other mixtures for sorption machines are lithium bromide–water and ammonia–water. The main advantages of the mixture TFE–E181 compared with the mixture LiBr–H_2O are complete miscibility in a wide temperature range, no corrosion and thermal stability up to 523 K. The working pressure in the range between 70 and 160 kPa is usually lower than that of the mixture NH_3–H_2O.

The one-stage process is shown in a p, T-diagram, *figure 1*. In the generator G the lower volatile refrigerant TFE and a small amount of absorbant E181 is desorbed from the rich solution (7). A heat flow $\dot{Q}_G$ is added at low pressure p_0 and at an intermediate temperature T_1. The refrigerant vapour (8) is precooled in the heat exhanger HXC (9) and then totally liquified in the condenser C by removing the heat flow $\dot{Q}_C$ at low pressure p_0 and ambient temperature T_0 (10). The refrigerant is then pumped by pump P_2 from the condenser C through the preheater HXC (11–12) into the evaporator E (12). By adding the heat flow $\dot{Q}_E$ at an intermediate temperature T_1 the refrigerant is evaporated. As reported by Hengerer and Stephan [3] small amounts of E181 coming from the generator with stream (12) cannot be completely evaporated in the evaporator and therefore would accumulate in this apparatus. In order to avoid such an accumulation of the absorbent E181 in the evaporator a reflux from the evaporator to the generator had to be installed (15). The weak solution from the generator (1) is pumped by pump P_1 through the solution heat exchanger HXS (2–3) into the absorber. The refrigerant vapour (13) is also fed into the absorber A where it is absorbed by the weak solution (3). The absorption process delivers a useful heat flow $\dot{Q}_A$, removed in the absorber at a pressure p_1 and a higher temperature T_2. The rich solution (4) leaves the absorber A and enters the solution heat exchanger HXS, where it preheats the weak solution (4–5). After mixing with the reflux of the evaporator E (6) the rich solution is throttled into the generator G, where the desorption of TFE takes place as described above.

2. EXPERIMENTAL SETUP

2.1. External cycles and controls

For testing compact brazed plate heat exchangers in the heat transformer, a test rig with a maximum heat input of 21 kW was designed and constructed. The experimental setup of the device is shown in *figure 2*.

Three control circuits were installed to keep the external process temperatures constant during the experiments. A liquid stream of hot water delivers the waste heat as driving force of the heat transformer. The temperature of the hot water stream (TICA13) is controlled by regulating the power of the electric heating H1. The main hot water stream is split off into two substreams, one heating the evaporator W1 and the other the generator W3. Part of the hot water reflux-stream from the generator is heated again in the heat exchanger W5, where the useful heat is removed from an oil stream passing through the absorber A1. The useful heat from the rich solution in the absorber is removed by oil, circulating between the heat exchanger W5 and the absorber A1. The temperature of the rich solution (TICA25) is controlled by the cooling fluid in the secondary circuit of the heat exchanger W5. Depending on the amount of useful heat removed from the rich solution, the flow of the cooling fluid is regulated by means of the air motor control valve VD2. The heat of condensation is delivered to the cold water, circulating between the condenser W6 and the heat exchanger W8. The water inlet temperature of the condenser W6 (TIC19) is controlled by regulating the external flow of cold water by air motor control valve VD3.

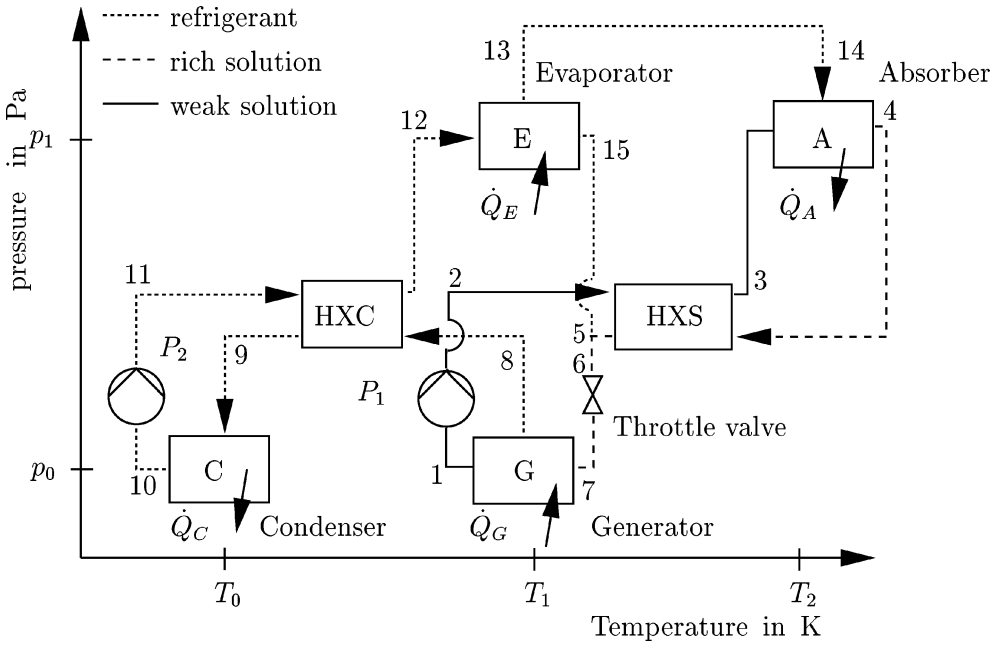

Figure 1. Principle of a one-stage absorption heat transformer.

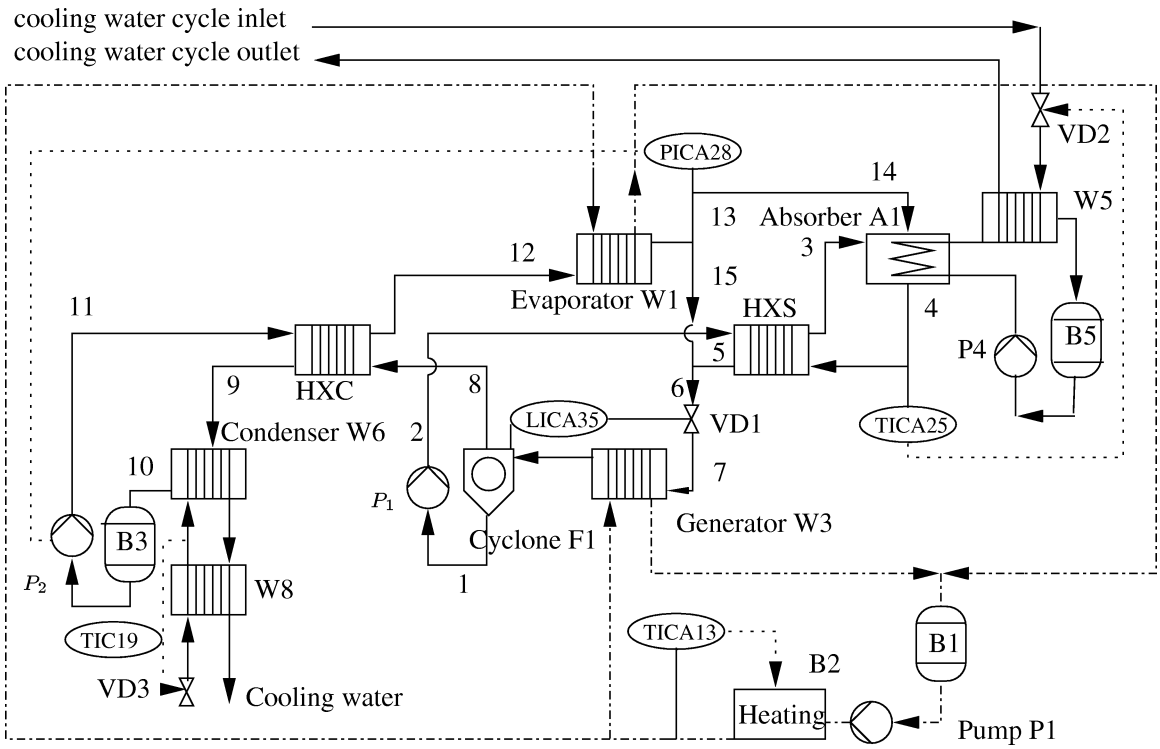

Figure 2. Scheme of the experimental setup.

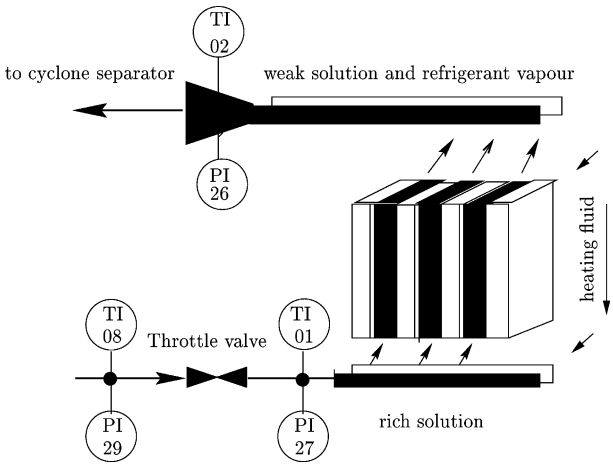

Figure 3. Scheme of the generator.

2.2. Internal cycles and controls

Compact brazed plate exchangers were used to reduce the investment costs of generator W3, evaporator W1, condenser W6, solution heat exchanger W4 and heat exchanger W5. Compared to shell and tube heat exchangers, plate heat exchangers offer some advantages: compact construction with a high area density, defined as the ratio of the heat transfer surface area to the heat exchanger volume. Typical values for plate heat exchangers are 100–200 m^{-1}. In some cases the ratio may rise up to 1000 m^{-1}. Conventional shell and tube heat exchangers reach values of 25–50 m^{-1}. Plate heat exchangers permit high overall heat transfer coefficients with a high heat capacity per volume, and the liquid hold-up is low.

We used a plate heat exchanger manufactured with rectangular plates, with four openings at the edges where two fluids pass alternating through the channels. The countercurrent flow scheme, *figure 3*, is effected by arrangement of the plates. Because of the shape of the plates small channels are formed with turbulent flow inside. The embossed surface provides a large heat transfer area on either side of the plates. The heat transfer surface looks like a herring-bone corrugation in flow direction. The generator W3 works as a climbing-film apparatus. The rich solution is throttled through the bottom inlet into a distribution chamber of the plate heat exchanger. It is evaporated as it passes upwards through the plates. The two-phase flow of vapour and liquid through the plates passes on top in a collector chamber and is afterwards separated in the cyclone F1.

The vapour from the generator W3 flows outside the helical coil heat exchanger HXC W2 and is totally

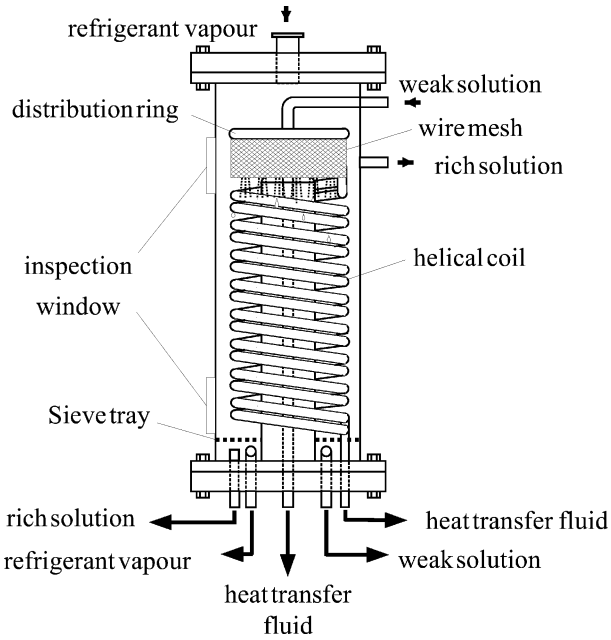

Figure 4. Sketch of the absorber.

liquified in condenser W6. The liquid refrigerant is stored in reservoir B3, and from there pumped by the gear pump P_2 through the heat exchanger HXC W2 into the evaporator W1. The mass flow rate of the refrigerant and the pressure PICA28 in the evaporator W1 are controlled by the revolutions of pump P_2. The mass flow can be varied between 0.01 $kg{\cdot}s^{-1}$ and 0.03 $kg{\cdot}s^{-1}$. The weak solution contains a mass fraction of 9 to 18 % TFE, and is pumped from the reservoir of cyclone F1 by the gear pump P_3 through the solution heat exchanger HXS into the absorber A1, *figure 4*. In the absorber A1, consisting of a stainless steel helical coil, the weak solution trickles down as a falling film over the sandblasted surface of the tubes. The weak solution enters through small orifices of a distribution ring onto a wire mesh leading the liquid to the first coil, *figure 4*. The mass flow rate of the weak solution could be varied by the gear pump P_3 between 0.095 $kg{\cdot}s^{-1}$ and 0.12 $kg{\cdot}s^{-1}$. Two inspection windows permitted a visual observation of the falling film. A narrow gap between two coils guaranteed a coherent laminar film. The absorber could be operated in different modes, either cocurrent or countercurrent flow of refrigerant and weak solution. The rich solution with mass fraction of 20 to 31 % TFE leaving the absorber A1 was precooled in the solution heat exchanger HXS W4 and throttled in control valve VD1 before entering the generator W3. The liquid level LICA35 of the cyclone separator F1 was held constant by means of the throttling

valve VD1. Thus flow fluctuations in the solution circuit could be avoided.

2.3. Measuring equipment

All external and internal process temperatures at the inlet and outlet of the apparatus as well as flow rates, pressures and liquid levels were recorded. Temperatures were measured with PT100 resistance temperature detectors, pressures with electronic pressure transmitters. Flow rates of the internal and external streams were continuously measured by flowmeters. The mass fractions of the rich and weak solutions and refrigerant were calculated from the density of a liquid sample. The density of the mixture was analyzed batchwise by a gravimetric method. The mass fraction was obtained iteratively from an equation of state $\xi^{\mathrm{L}} = \xi^{\mathrm{L}}(p, T, \rho)$ [9].

3. EXPERIMENTS AND RESULTS

3.1. Experimental conditions and coefficients

Experiments were conducted with a constant hot water inlet temperatures of 363.15 K and a constant condensation temperature of 293.15 K. The temperature of the rich solution was varied in the experiments by means of the control TICA25. Thus the temperature lift ΔT, defined as the difference between the temperatures of the rich solution leaving the absorber and the weak solution leaving the generator, could be varied as well. The parameters, such as coefficient of performance COP, specific solution ratio f and overall heat transfer coefficients k were determined by internal mass and energy balances of the specific apparatus. The COP of the one-stage process is defined as

$$\mathrm{COP} = \zeta = \frac{|\dot{Q}_{\mathrm{A}}|}{|\dot{Q}_{\mathrm{G}}| + |\dot{Q}_{\mathrm{E}}|} \tag{1}$$

The specific solution ratio f was calculated as the ratio of the mass flows of the rich solution and the refrigerant. It may also be calculated by mass fractions of the internal streams or the mass fraction spread $\Delta\xi$ according to

$$f = \frac{\dot{m}_{\mathrm{r}}}{\dot{m}_{\mathrm{R}}} = \frac{\xi_{\mathrm{R}} - \xi_{\mathrm{w}}}{\xi_{\mathrm{r}} - \xi_{\mathrm{w}}} = \frac{\xi_{\mathrm{R}} - \xi_{\mathrm{w}}}{\Delta\xi} \tag{2}$$

The specific reflux ratio f_{re} in the evaporator is the ratio of the mass flows of the not evaporated liquid leaving the evaporator, and the total amount of refrigerant fed into the apparatus. Besides those coefficients the heat ratio ψ is defined as the ratio of the heat fluxes transferred in the solution heat exchanger and the absorber. The overall heat transfer coefficient k was determined with the logarithmic mean temperature difference $\Delta\vartheta$, the heat flow $\dot{Q}$ and the heat exchanger area A:

$$k = \frac{\dot{Q}}{A\Delta\vartheta} \tag{3}$$

wherein the logarithmic mean temperature difference $\Delta\vartheta$ is given by

$$\Delta\vartheta = \frac{\Theta_{\mathrm{i}} - \Theta_{\mathrm{o}}}{\ln(\Theta_{\mathrm{i}}/\Theta_{\mathrm{o}})} \tag{4}$$

Θ_{i} is the temperature difference of the fluids at the inlet, and Θ_{o} at the outlet of the apparatus. Analogous to the overall heat transfer coefficient we can define an overall mass transfer coefficient β for the generator and the absorber with the logarithmic mean mass fraction difference $\Delta\Upsilon$, the transferred mass flux $\dot{m}$ and the area A:

$$\beta = \frac{\dot{m}}{A\Delta\Upsilon} \tag{5}$$

The logarithmic mean mass fraction difference $\Delta\Upsilon$ is defined as

$$\Delta\Upsilon = \frac{\Delta\xi_{\mathrm{o}} - \Delta\xi_{\mathrm{i}}}{\ln(\Delta\xi_{\mathrm{o}}/\Delta\xi_{\mathrm{i}})} \tag{6}$$

$\Delta\xi_{\mathrm{o}}$ and $\Delta\xi_{\mathrm{i}}$ are the mass fraction differences between the equilibria mass fractions and the measured mass fractions at the inlet and at the outlet of the apparatus. Another characteristic coefficient for the falling film absorber is the Reynolds number Re_{F}, defined as

$$Re_{\mathrm{F}} = \frac{\dot{m}_{\mathrm{w}}}{U\eta} \tag{7}$$

Herein U is the perimeter of the tube circumference of the helical coil covered with liquid, $\dot{m}_{\mathrm{w}}$ the mass flux of the weak solution and η the dynamic viscosity of the weak solution.

3.2. Results and discussion

In *figure 5* the calculated and measured COPs are plotted versus the internal temperature lift ΔT. For steady operation in the experiments a maximum COP of 0.42 is reached for a temperature lift of 18 K from

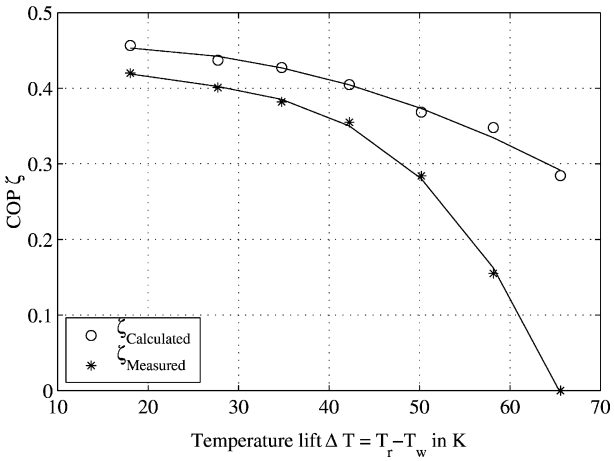

Figure 5. Measured and calculated COP versus temperature lift for a temperature of the weak solution of 348.2 K and a condensation temperature of 293.15 K.

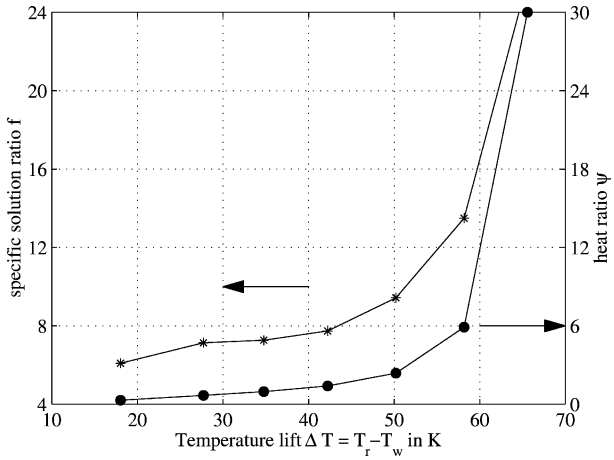

Figure 6. Specific solution ratio f and heat ratio ψ versus temperature lift for a temperature of the weak solution of 348.2 K and a condensation temperature of 293.15 K.

TABLE I
Input parameters for the calculation of the process.

temperature of the rich solution	variable
temperature of the weak solution	348.2 K
condensation temperature of the refrigerant	293.15 K
absorber efficiency	0.5–0.6
generator efficiency	0.6–0.7
temperature difference solution heat exchanger HXS (points 4, 3 in *figure 1*)	0.7–1.8 K
temperature difference heat exchanger HXC (points 9, 11 in *figure 1*)	38–40 K

348.2 K to 366.2 K. The COP is lower for a higher temperature lift. Experimental and calculated values, determined with a steady-state thermodynamic model, described by Hengerer and Stephan [3] agree well. The model takes into account the measured temperatures, efficiencies of absorber and generator due to incomplete absorption or desorption, pressure drop in the apparatus and tubes, and the temperature differences for HXC and HXS. *Table I* gives typical values for these input parameters. The calculated COP values, based on these measured input variables, are about 10 % higher than measured. The differences become significant, *figure 5*, when temperature lifts are above 50 K. This behavior is caused by a high specific reflux ratio f_{re}, because of a high amount of not evaporated liquid accumulated in the evaporator. The calculated values of the TFE mass fractions in the refrigerant flowing to the evaporator were slightly lower in the experiments. Measured COP values hence were lower than the calculated values. This effect increases with higher temperature lifts.

The COP decreases with the temperature lift because of a higher specific solution ratio f, *figure 6*, left ordinate. The ratio f increases with the flow rate of the absorbent circulating between absorber and generator. With higher flow rate the mass fraction spread $\Delta\xi$ becomes smaller. As an analysis of liquid samples revealed, the mass fractions of the weak solution and the refrigerant remained almost constant, because the process parameters of the condenser and the generator did not change. Only the mass fraction of the rich solution decreases with the temperature of the rich solution. In a similar way the heat ratio ψ increases with temperature lifts, *figure 6*, right ordinate. The rich solution leaving the absorber reaches higher temperatures the more heat is transferred in the solution heat exchanger. Then the heat released in the absorber and the COP decrease. In the limiting case when the highest temperature of the rich solution is reached, no heat will be released and the heat ratio ψ tends to infinity.

The simulation with the steady-state thermodynamic model also revealed that the heat transformer COP of TFE–E181 under the same conditions is always about 1.05–1.10 higher than the values obtained with ammonia–water as working pair, *table II*. The mixture TFE–E181 in an absorption heat transformer is therefore a good alternative to ammonia–water, all the more as working pressures are much lower, and hence also the investment costs. Also the liquid pumps are smaller and easier to operate. A rectification in the generator is not necessary. The COP values for the mixture lithium bromide–water turned out to be by approximately 15–20 % higher than those with TFE–E181, *table II*. However, the temperature lift when working with lithium bromide–water is limited

TABLE II
Comparison of calculated COP values for different working pairs.

T_r (absorber outlet) in K	ζ for TFE–E181	ζ for NH_3–H_2O	ζ for LiBr–H_2O
399.3	0.3685	0.3431	0.5005
391.13	0.4049	0.3548	0.5025
382.68	0.4275	0.363	0.5040
374.34	0.4371	0.3717	0.5046

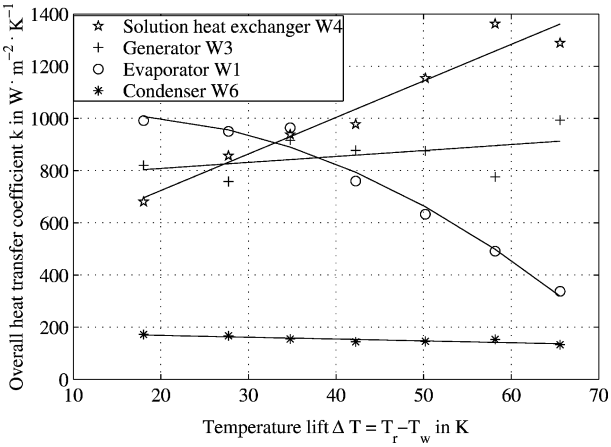

Figure 7. Overall heat transfer coefficients versus temperature lift for different plate heat exchangers.

to 45–50 K due to the risk of crystallization of the solution in the generator. When the temperature of the rich solution is high, a large amount of solution circulates between absorber and generator due to the small spread of mass fractions. Another disadvantage of the mixture lithium bromide–water are the massive problems with pitting corrosion of steel.

3.3. Heat and mass transfer coefficients

3.3.1. Plate heat exchangers

As *figure 7* shows, the overall heat transfer coefficients depend on the temperature lift. The thermophysical properties like the dynamic viscosity η, the density ρ, the specific heat capacity c_p, and the thermal conductivity λ depend on the temperature and the mass fraction of the solution. Other important parameters are, e.g., the velocity of the fluid or the geometry and structure of the plate surface. According to the experiments, the overall heat transfer coefficient k for the solution heat exchanger increased from 700 to 1350 $W \cdot m^{-2} \cdot K^{-1}$ with higher temperature lifts. This is mainly due to the

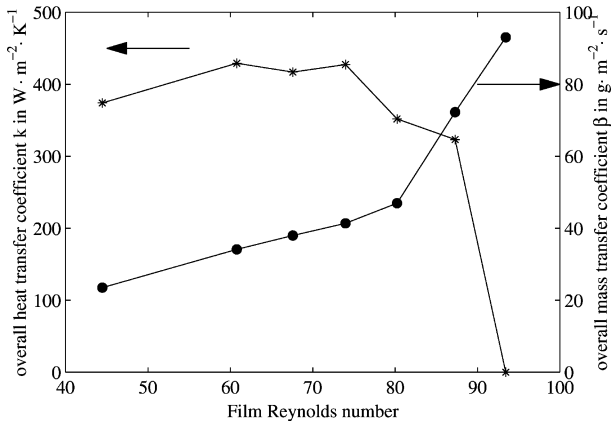

Figure 8. Overall heat and mass transfer coefficients versus Reynolds number for the falling film absorber.

smaller dynamic viscosity caused by the rising temperature of the rich solution. Another reason is the rising mass flux of the rich solution, leading to a higher flow velocity inside the apparatus. The overall heat transfer coefficients of the evaporator show a decreasing trend from 1000 $W \cdot m^{-2} \cdot K^{-1}$ to 300 $W \cdot m^{-2} \cdot K^{-1}$ with the temperature lift, affected by the smaller refrigerant flow rate. The k-value of the condenser remains nearly constant at 180 $W \cdot m^{-2} \cdot K^{-1}$, and is independent from the temperature lift. The k-value of the generator lies in the range of 750 and 1000 $W \cdot m^{-2} \cdot K^{-1}$, with a slightly ascending trend with higher temperature lifts, because of the higher solution flow rate.

Table III shows experimental results of the overall mass transfer coefficient β_G for different temperatures and mass fractions of the rich solution at the inlet of the generator, β_G being in the range between 133 and 233 $g \cdot m^{-2} \cdot s^{-1}$. It increases with rising temperature and descending mass fraction of the rich solution at the inlet of the generator. These two variables lead to an increase of the diffusion coefficient of the rich solution of about 15 %. The dynamic viscosity decreases about 12 %, *table III*. Both fluid properties have a positive influence on the overall mass transfer coefficient, because they minimize the mass transfer resistance on the liquid side.

3.3.2. Falling film absorber

The experimental results of the overall heat and mass transfer coefficients of the absorber are plotted in *figure 8* versus the Reynolds number of the falling film. Increasing Reynolds numbers in *figure 8* are synonymous with increasing temperatures of the rich solution leaving the absorber. Both k_A and β_A, show an opposite tendency with increasing Reynolds numbers. For low

TABLE III
Overall mass transfer coefficient of the generator and fluid properties of the rich solution at the generator inlet for different process conditions.

T_r in K	$\xi_r^{measured}$	β_G in g·m^{-2}·s^{-1}	D in m^2·s^{-1}	η in kg·m^{-1}·s^{-1}
360.16	0.2516	233.1	$2.7614 \cdot 10^{-9}$	0.0010784
358.31	0.256	165.6	$2.6725 \cdot 10^{-9}$	0.0011054
357.45	0.2546	159.6	$2.6319 \cdot 10^{-9}$	0.0011164
357.02	0.2476	142.0	$2.6118 \cdot 10^{-9}$	0.0011170
355.68	0.2565	133.3	$2.5498 \cdot 10^{-9}$	0.0011421
353.29	0.2732	147.8	$2.4417 \cdot 10^{-9}$	0.0011876

TABLE IV
Alteration of the thermophysical mixture properties depending on the temperature of the rich solution at the absorber outlet.

T_r in °C	Re_F	η in kg·m^{-1}·s^{-1}	D in m^2·s^{-1}	λ in W·m^{-1}·K^{-1}
415.14	93.43	0.0005696	$6.4533 \cdot 10^{-9}$	0.1269
407.26	87.28	0.000642	$5.7876 \cdot 10^{-9}$	0.1269
399.3	80.23	0.0007137	$5.165 \cdot 10^{-9}$	0.1271
391.13	73.98	0.0007817	$4.5755 \cdot 10^{-9}$	0.1279
382.68	67.59	0.0008587	$4.0164 \cdot 10^{-9}$	0.1287
374.34	60.79	0.0009459	$3.513 \cdot 10^{-9}$	0.1294
365.45	44.46	0.0010497	$3.0269 \cdot 10^{-9}$	0.1301

Reynolds numbers up to 80 the overall heat transfer coefficient k_A is in the range between 370 W·m^{-2}·K^{-1} and 430 W·m^{-2}·K^{-1}. It decreases with higher Reynolds numbers, while the overall mass transfer coefficient β_A increases from 20 g·m^{-2}·s^{-1} to 90 g·m^{-2}·s^{-1} at the highest Reynolds number. The total amount of heat released in the absorber is close to zero at the highest temperature of the rich solution, it increases with lower temperatures. In addition, also the mass fraction of the solution and also the refrigerant mass flux fed into the absorber decrease.

On the other hand the temperature of the rich solution influences also the thermophysical transport properties of the working mixture, as shown for the absorber in *table IV*. With rising temperature of the rich solution the dynamic viscosity becomes smaller and hence the Reynolds number of the falling film, defined in equation (7), rises. The combined effect of these parameters leads to a thinner film on the surface of the helical coil. Hence the main heat and mass transfer resistances on the liquid side of the film are reduced, as confirmed by the results of *figure 8* and *table IV*.

Another important reason for the increase of the overall mass transfer coefficient is the strong, almost twofold, increase of the diffusion coefficient with higher Reynolds numbers and higher temperatures of the rich solution. In conjunction with the lower film thickness the mass transfer resistance on the liquid side becomes smaller, leading to an increase of the overall mass transfer coefficient β_A, *figure 8*. The overall heat transfer coefficient, however, decreases with rising Reynolds numbers, because of the lower heat flux. The influence of the thermal conductivity λ on the overall heat transfer coefficient is not as significant as that of the diffusion coefficient on the overall mass transfer coefficient.

3.3.3. Comparison of the apparatus types

Experiments with the falling film absorber and the compact plate heat exchangers showed for the overall heat and mass transfer coefficients a dependence on the process temperature of the rich solution. The generator, built as a plate heat exchanger, enables higher heat and mass flux densities with higher overall transfer coefficients for desorption compared to the falling film absorber. Plate heat exchangers offer several advantages because of their compact structure. Different from a falling film apparatus they do not require a good distribution device for the liquid, when liquid and gaseous phase flow cocurrently over the heat and mass transfer surface. The herringbone surface structure of the plate heat exchangers guarantees an intensive mixing of the two-phase flow and hence an intensive heat and mass transfer. Unlike falling

films the turbulent mixing and fluid flow together with the static height in the generator leads to an additional pressure drop in the order of 12–15 kPa. For that reason the entrance temperature of the rich solution entering the generator is not as low as if there was no pressure drop across the generator. With the simulation program we investigated the influence of the generator pressure drop on the performance of the process. The results showed that this yields a slightly higher COP for the process at a lower temperature of the weak solution leaving the generator due to the inevitable pressure drop. The results revealed also that the amount of useful heat released in the absorber for the same mass flux of the weak solution is about 2 % lower with a pressure drop in the generator.

The calculated k-values of the generator and evaporator are about 30 % higher compared to shell and tube heat exchangers. Hence for a given heat flow and logarithmic mean temperature difference the required heat exchanger area is 77 % of that of a shell and tube exchanger. This leads together with the high volumetric area of the plate heat exchangers of 50–100 m^{-1} to a reduction of the apparatus volume and size. As a consequence the investment costs for the generator and evaporator are 70 % lower according to statements of the manufacturers. Thus the total investment costs could be reduced to about 20 %.

The overall heat transfer coefficient of the helical coil absorber is nearly twice as high as that of a comparable horizontal tube absorber. Thus, the helical coil absorber needs only half the space of a horizontal tube absorber.

4. SUMMARY

The steady-state operation of the absorption heat transformer, working with the mixture TFE–E181, was analyzed for different temperatures of the rich solution. A maximum COP of 0.42 was reached for an internal temperature lift from 348.2 K to 366.2 K. The COP decreases with higher temperatures of the rich solution. Heat and mass transfer coefficients for the generator and absorber were measured and presented for different process parameters. The use of compact brazed plate heat exchangers as generator, evaporator, condenser and solution heat exchanger instead of shell and tube heat exchangers leads to higher overall heat transfer coefficients and therefore to a reduction of the heat exchanger size and hence the total investment costs. A considerable reduction of the required heat exchanger area of the falling film absorber, when built as helical coil absorber, can be achieved compared with the usual horizontal tube absorber.

The tests of the equipment showed also the suitability of the working mixture TFE–E181 for use in absorption heat transformers. The experimental results agree well with computer calculations. As the calculated results showed, the working pair TFE–E181 leads at least to the same or higher COP values as ammonia–water. The mixture TFE–E181 hence is a good alternative for the use in absorption heat transformers.

Acknowledgements

The authors are indebted to the Bundesministerium für Bildung, Wissenschaft, Forschung und Technologie (BMBF), Bonn, and GEA AG, Herne, for financial support of this project. We also gratefully acknowledge the supply of E181 by former Hoechst AG, Burgkirchen (now Clariant AG).

REFERENCES

[1] Seher D., Stephan K., Trifluorethanol als Arbeitsstoff für Absorptionswärmepumpen und Absorptionswärmetransformatoren, Klima-Kälte-Heizung 7–8 (1983).

[2] Seher D., Stephan K., Comparison of working substances for heat transformer cycles, VDI Berichte 539 (1984) 133–162.

[3] Stephan K., Hengerer R., Heat transformation with the ternary working fluid TFE–H_2O–E181, Internat. J. Refrigeration 16 (2) (1993) 120–128.

[4] Seher D., Arbeitsstoffgemische für Absorptionswärmepumpen und Absorptionswärmetransformatoren, Dissertation, Universität Stuttgart, 1985.

[5] Lopez E.R., Garcia J., Legido J.L., Coronas A., Fernandez J., Experimental and predicted excess enthalpies of the 2,2,2-trifluoroethanol–water–tetraethyleneglykoldimethylether ternary system using binary mixing data, J. Chem. Soc. Faraday Trans. 91 (14) (1995) 2071–2079.

[6] Coronas A., Valles M., Chaudari S.K., Patil K.R., Absorption heat pump with the TFE–TEGDME and TFE–H_2O–TEGDME systems, Appl. Thermal Engrg. 16 (4) (1996) 335–345.

[7] Coronas A., Valles M., Chaudhari S.K., Thermodynamic analysis of a double-effect absorption cycle working with TFE–TEGDME for air-conditioning, Appl. Thermal Engrg. (1998).

[8] Boer D., Valles M., Coronas A., Performance of double effect absorption compression cycles of air-conditioning using methanol–TEGDME and TFE–TEGDME systems as working pairs, Internat. J. Refrigeration 21 (7) (1998) 542–555.

[9] Seher D., Stephan K., Sorptionswärmepumpe Stoffsysteme, Institut für Thermische Verfahrenstechnik und Technische Thermodynamik, Universität Stuttgart, 1985.